

# Temporal Scaling Law for Large Language Models

Yizhe Xiong<sup>1,2</sup> Xiansheng Chen<sup>3</sup> Xin Ye<sup>3</sup> Hui Chen<sup>1,2</sup> Zijia Lin<sup>3</sup>  
 Haoran Lian<sup>4</sup> Zhenpeng Su<sup>5</sup> Jianwei Niu<sup>4</sup> Guiguang Ding<sup>1,2</sup>

<sup>1</sup>Tsinghua University

<sup>2</sup>Beijing National Research Center for Information Science and Technology (BNRist)

<sup>3</sup>Kuaishou Technology <sup>4</sup>Beihang University

<sup>5</sup>Institute of Information Engineering, Chinese Academy of Sciences, Beijing, China

{xiongyizhe2001, yexin0807}@gmail.com chenxiansheng@pku.edu.cn

huichen@mail.tsinghua.edu.cn {lianhaoran, niujianwei}@buaa.edu.cn

linzijia07@tsinghua.org.cn dinggg@tsinghua.edu.cn suzhenpeng@iie.ac.cn

## Abstract

Recently, Large Language Models (LLMs) have been widely adopted in a wide range of tasks, leading to increasing attention towards the research on how scaling LLMs affects their performance. Existing works, termed Scaling Laws, have discovered that the final test loss of LLMs scales as power-laws with model size, computational budget, and dataset size. However, the temporal change of the test loss of an LLM throughout its pre-training process remains unexplored, though it is valuable in many aspects, such as selecting better hyperparameters *directly* on the target LLM. In this paper, we propose the novel concept of Temporal Scaling Law, studying how the test loss of an LLM evolves as the training steps scale up. In contrast to modeling the test loss as a whole in a coarse-grained manner, we break it down and dive into the fine-grained test loss of each token position, and further develop a dynamic hyperbolic-law. Afterwards, we derive the much more precise temporal scaling law by studying the temporal patterns of the parameters in the dynamic hyperbolic-law. Results on both in-distribution (ID) and out-of-distribution (OOD) validation datasets demonstrate that our temporal scaling law accurately predicts the test loss of LLMs across training steps. Our temporal scaling law has broad practical applications. First, it enables direct and efficient hyperparameter selection on the target LLM, such as data mixture proportions. Secondly, viewing the LLM pre-training dynamics from the token position granularity provides some insights to enhance the understanding of LLM pre-training.

## 1 Introduction

Large Language Model (LLM) marks a paradigm shift in the scope of natural language processing, demonstrating unprecedented capabilities in accomplishing complicated tasks of natural language understanding and generation (Devlin et al., 2019;

Radford et al., 2018). A cornerstone of this remarkable progress lies in the scalability of the Transformer architecture (Vaswani et al., 2017), which has facilitated the development of increasingly large models. Moreover, the accessibility of large-scale training is significantly enhanced by the abundance of data gathered from the Internet, which enables the construction of giant training datasets to improve model performance (Radford et al., 2019). Due to the scalability of both the model size and training data scale, LLMs with billions of parameters (Brown et al., 2020) and even trillions of parameters (Fedus et al., 2022) are widely proposed and applied in various tasks.

The scalability of LLMs has been extensively studied in terms of variables like model size, computational budget, and dataset size (Kaplan et al., 2020). Prior works in this domain, which are commonly referred to as “scaling laws” (Kaplan et al., 2020; Henighan et al., 2020), have proposed empirical principles to characterize the power-law (i.e., exponential patterns) among those variables. Those scaling laws demonstrate that the final test loss of an LLM improves exponentially with scalable factors, i.e., model size, computational budget, and dataset size. Recently, similar explorations have expanded to multi-modal training (Cherti et al., 2023; Aghajanyan et al., 2023) and transfer learning (Hernandez et al., 2021), enabling researchers to predict the performance of LLMs in different scenarios.

Prior works of scaling laws typically predict the final test loss of *fully-trained LLMs with a given computational budget* after completing their pre-training *with mostly fixed hyperparameters* (e.g., data mixture proportions, weight decay, etc.) (Kaplan et al., 2020; Henighan et al., 2020; Cherti et al., 2023; Aghajanyan et al., 2023). However, variations in training hyperparameters also significantly influence the final test loss in a complicated way (Yang et al., 2022; Xie et al., 2023a). That underscores the need for a more fine-grained scaling

law, which can *predict the temporal evolution of the test loss as training steps scale up under different training hyperparameters* on a fixed model size and data scale. Such a temporal scaling law is complementary to prior works, because it further enables the identification of better training hyperparameters, such as data configurations and learning rates, after the model size and data scale are determined based on previous research. Considering that many current LLMs are trained with hyperparameters selected on a much smaller one due to computational costs, our work addresses the recognized issue that hyperparameters like data mixture proportions (Xie et al., 2023b) and regularization hyperparameters (Yang et al., 2022) are not always transferrable from a small language model to a much larger one, via proposing a two-stage pipeline to directly select hyperparameters on the target LLM. Furthermore, such a temporal scaling law provides a theoretical basis for studying some training dynamics of LLMs. Despite the broad applications, prior works have not explored practical scaling laws from the temporal perspective.

In this paper, we propose the novel concept of **Temporal Scaling Law** for Large Language Models. Specifically, we first try to model the test loss as a whole in a coarse-grained manner but find it to be not precise enough. Then we further break the test loss into the losses for tokens in different positions. And by careful investigation, we discovered that the losses on different token positions conform to a dynamic hyperbolic-law across different training steps. We further examine the evolution of the curve parameters for the dynamic hyperbolic-law and identify their temporal patterns. We term this phenomenon as the temporal scaling law, i.e., *how the test loss of an LLM evolve as the training steps scale up*. Our temporal scaling law accurately predicts the subsequent test losses using the data from an early training period. Prediction results on both the in-distribution (ID) and the out-of-distribution (OOD) validation datasets show that our methodology significantly improves over baseline approaches.

Our temporal scaling law has broad practical applications for LLM pre-training. In this paper, we provide two use cases as examples. First, our temporal scaling law presents a novel and practical approach to selecting the hyperparameters *directly on the target to-be-pre-trained LLM*. Taking the data mixture proportion as an example, current works generally tune data proportions on a small-

scale model and directly apply the tuned weights to pre-training the much larger target LLM (Xie et al., 2023a). However, optimal hyperparameters for a small-scale model probably are not the optimal ones for the much larger target LLM (Yang et al., 2022), though they can be effective candidates. With the accurate loss prediction from our proposed temporal scaling law, we can leverage a two-stage pipeline to better select the target LLM’s hyperparameters, i.e., firstly using a small model to narrow down the range of candidate hyperparameter values and then directly selecting the best one which can achieve the best predicted test loss after training the target LLM with it for a small-scale of training data. Second, our temporal scaling law reveals some learning dynamics of LLMs at the token granularity. Specifically, we discovered that the loss decrease rate for tokens on different positions remains uniform after an early training period. Through experiments on various position-based weighting strategies, we verify the effectiveness of the default pre-training practice, in which no weighting strategies on different token positions are applied, though they are imbalanced in terms of learning difficulty.

Overall, our contributions are threefold:

- First, we propose the Temporal Scaling Law for LLMs, modeling the evolution of test loss during the LLM pre-training process.
- Second, based on our proposed temporal scaling law, we provide a method for precisely predicting the subsequent test losses after deriving the parameters of the temporal scaling law from an early training period.
- Lastly, we present two scenarios to illustrate the broad practical applications of our temporal scaling law. For hyperparameter tuning, our temporal scaling law enables the direct selection of better hyperparameter values based on predicted LLM performance on the target LLM. For learning dynamics, our temporal scaling law provides theoretical and experimental verifications for the default pre-training practice that puts no weights on each token loss at different positions.

## 2 Related Works

### 2.1 Large Language Models

Language models are statistical models designed to model the probabilistic correlation in natural lan-

guage sequences (Touvron et al., 2023a). The introduction of the Transformer architecture (Vaswani et al., 2017) led to the development of large language models. GPT-3 (Brown et al., 2020) marks the beginning of the LLM era, as decoder-based generative models are capable of completing various tasks via in-context learning. Further advancements in LLMs include PaLM (Chowdhery et al., 2023), Pythia (Biderman et al., 2023), LLaMA (Touvron et al., 2023a), etc. Currently, GPT-4 (OpenAI, 2023) has pushed the boundaries of LLMs further in terms of scale and capability.

## 2.2 Scaling Laws for Language Models

The concept of scaling laws for language models was proposed by (Kaplan et al., 2020). Their study revealed that the test loss for generative transformer models scales as a power-law with model size, dataset size, and the amount of computation used for training. Building upon that foundational study, further research has expanded the concept of scaling laws to diverse problem settings (Hernandez et al., 2021) and model architectures (Cherti et al., 2023; Aghajanyan et al., 2023). For instance, (Hernandez et al., 2021) has investigated scaling laws for transfer learning. (Cherti et al., 2023) and (Aghajanyan et al., 2023) observed scaling laws for multi-modal model pre-training.

Despite previous advancements, a critical point that remains underexplored is the temporal trajectory of LLM performance throughout training. According to (Kaplan et al., 2020), when LLMs are pre-trained with infinite data and training steps, the test loss follows the power-law. However, this assumption cannot be fulfilled in real-world, thus the power-law may not be accurate to portray the temporal pattern of test loss during actual pre-training. By studying the loss behavior on different token positions, we introduce temporal scaling law, allowing for more precise tracking and prediction of LLM test loss during pre-training.

## 3 Temporal Scaling Law

### 3.1 Preliminaries

**Pre-training Language Models.** We mainly discuss the generation process of decoder-based generative language models. A generative language model is trained via next-token prediction. During the pre-training process, the text corpus is commonly segmented into token sequences with an identical length. The token sequences are then

fed to the model for calculating the prediction loss on each token position  $i$ . Formally, given a training text sequence  $T_n$  consisting of  $n$  tokens, i.e.,  $T_n = [t_1, \dots, t_{i-1}, t_i, \dots, t_n]$ , when predicting the token  $t_i$ , the language model takes the previous tokens  $T_{i-1} = [t_1, \dots, t_{i-1}]$  as input, and generates the probability distribution  $\mathbf{p}_i$  for the token  $t_i$ . The loss  $\mathcal{L}_i$  w.r.t. the token  $t_i$  is commonly calculated via the cross-entropy loss function. In decoder-based transformers (Vaswani et al., 2017), a look-ahead mask is applied in the multi-head attention (MHA) module to ensure that each token can only attend to previous tokens, preserving the causal order of the generated sequence. Then, all tokens'  $\mathbf{p}_i$  are calculated in a single forward pass in parallel. The loss  $\mathcal{L}_i$  on each token's  $\mathbf{p}_i$  is then averaged as the loss for the sequence  $T_n$ :

$$\mathcal{L}_{T_n} = \frac{1}{n} \sum_{i=1}^n \mathcal{L}_i \quad (1)$$

### 3.2 Experiment Setup

We use experiment results to derive the temporal scaling law, and conduct predictions after deriving parameters of the temporal scaling law from an early training period. See Appendix for details.

**Train Dataset.** We train LLMs on the Pile (Gao et al., 2021), a large-scale, publicly available monolingual corpus in English for language model pre-training, consisting of 22 text domains. For all experiments, we tokenize it using the LLaMA tokenizer (Touvron et al., 2023a) with a 32k vocabulary. We apply the domain weights in (Su et al., 2023) for LLM pre-training.

**Validation Dataset.** We apply two validation datasets for test loss calculation. For the in-distribution (ID) dataset, we randomly sample 800 sequences (1024 consecutive tokens for each) for each text domain from the validation set in the Pile. For the out-of-distribution (OOD) dataset, we simply adopt the validation split of the RealNews-Like domain in the C4 dataset (Raffel et al., 2020), as it is claimed to be “distinct from the Pile” (Gao et al., 2021). We refer to both validation datasets as ID-Val and OOD-Val, respectively. When calculating test loss, we forward all sequences in the validation dataset and average the results. It is worth noting that calculating test loss is equivalent to calculating the perplexity (PPL) for the validation dataset since PPL can be directly acquired via test loss:

$$\text{PPL}(T) = \exp\left\{-\frac{1}{n} \sum_i^n \log p_\theta(t_i | T_{i-1})\right\} \quad (2)$$

Model	ID-Val		OOD-Val	
	Power-law	Ours	Power-law	Ours
468M	<b>-2.8746</b>	0.9988	<b>-2.7967</b>	0.9983
1.2B	<b>-2.3998</b>	0.9995	<b>-2.3780</b>	0.9993

Table 1:  $R^2$  results for fitting the test loss with the power-law and our temporal scaling law. Note that the fit is calculated on complete test loss data. The power-law **fails** in portraying the test loss evolution.

**Models.** We train two generative language models with 468M and 1.2B parameters, respectively. The architectures of models are identical to the 410M and 1.0B parameter models in (Biderman et al., 2023). The differences between model parameters can be ascribed to the different vocabulary sizes and different activation functions (i.e., SwiGLU v.s. GeLU). See Appendix for details.

**Training.** Following LLaMA (Touvron et al., 2023a), we apply the AdamW optimizer (Loshchilov and Hutter, 2019) with a learning rate of  $3e-4$ . Following most open-source LLMs (Touvron et al., 2023a; Biderman et al., 2023), we use the cosine learning rate decay schedule (Loshchilov and Hutter, 2017) for all experiments and set total warmup steps as  $1k$ . All models are pre-trained with 400B tokens.

**Metric for Fitting Model Evaluation.** We propose the temporal scaling law to fit the test loss during pre-training. Following the common practical choice (Cheng et al., 2014), we choose the coefficient of determination ( $R^2$ ) to evaluate the quality of the fit.  $R^2$  demonstrates the proportion of the variability in the ground-truth that the proposed fit could explain. Formally, we have:

$$R^2 = 1 - \frac{\sum_i (y_i - f_i)^2}{\sum_i (y_i - \bar{y})^2}, \quad (3)$$

where  $y_i$  is the ground-truth test loss w.r.t. the  $i$ -th step, and  $\bar{y}$  is the average of  $y_i$ .  $f_i$  is the fit test loss w.r.t. the  $i$ -th step.  $R^2 \in (-\infty, 1]$  and a perfect fit has  $R^2 = 1$ . A greater  $R^2$  indicates a better fit.

### 3.3 Temporal Scaling Law

The original scaling law (Kaplan et al., 2020) has validated that the temporal loss evolution of LLMs during pre-training follows a power-law under the assumption that training tokens are infinite and the LLM is trained with infinite training steps. However, in real-world applications, the maximum step of the training schedule is limited. To validate the effectiveness of the power-law in a limited training schedule, we pre-train 468M and 1.2B models

following Sec. 3.2, and fit the power-law function ( $\mathcal{L} = (p_1 x)^{p_2} + p_3$ ,  $\{p_i\}$  are fitting parameters) to the test loss evolution curve (i.e., treating test loss as a whole to fit in this case) using non-linear least squares. As shown in Tab. 1, applying the power-law results in negative  $R^2$  values, indicating that the power-law fails to portray the test loss evolution across model scales and validation datasets. Such results motivate us to find a better method to understand the test loss evolution under real-world limitations where training steps are limited during LLM pre-training.

**The Dynamic Hyperbolic-Law of Loss on Different Token Positions.** To fit and predict the test loss more precisely, we propose to break it down and investigate the temporal scaling law from a finer granularity and look into the inherent patterns of the loss on every token position. Language models are statistical models trained to model the probabilistic process of next-token prediction. Formally, for a sequence of  $n$  tokens  $T_n = (t_1, t_2, \dots, t_n)$ , the probability of the following token being  $t_{n+1}$  given the preceding tokens is denoted as  $P(t_{n+1}|t_1, t_2, \dots, t_n)$ . Intuitively and statistically, in a consecutive sequence:

$$\mathbb{E}[P(t_{n+1}|T_n)] \gtrsim \mathbb{E}[P(t_n|T_{n-1})], \quad (4)$$

since  $t_{n+1}$  has a longer context than  $t_n$ . To illustrate this pattern, we plot the results of test loss for tokens in different positions, as validated on our ID-Val, using both our 468M and 1.2B models after completing pre-training. As shown in Fig. 1, both models, although varying in scales, follow the same pattern that test loss for tokens with shorter context is commonly higher than that for tokens with longer context. For both models, the loss values for tokens near the end of the sequence seem to converge at a certain value. We find that this trend can be fit with a hyperbolic relation:

$$\mathcal{L}_i = \frac{a_0}{1 + a_1 i} + a_2, \quad (5)$$

where  $\mathcal{L}_i$  is the loss on token position  $i$  ( $1 \leq i \leq n$ ), and  $a_0$ ,  $a_1$ , and  $a_2$  are fitting parameters solved by non-linear least squares. The fit for data from our 468M and 1.2B model are presented in Fig. 1. By applying this fit to test loss results of all checkpoints across the training phase, we find that over 99% of them can be fit with such hyperbolic relation with  $R^2 > 0.95$ , well demonstrating its generality. We term this phenomenon as the dynamic

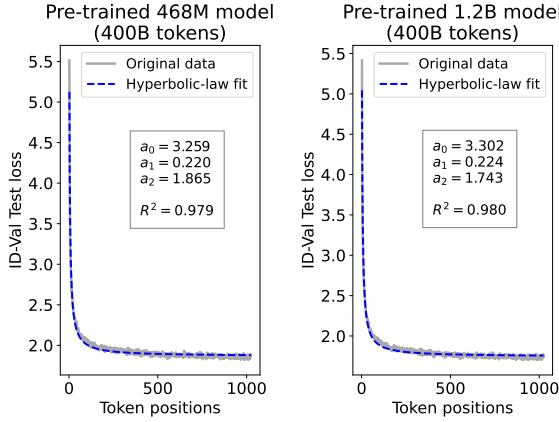


Figure 1: Graph of actual loss and fitting curve across different token positions for the 468M and 1.2B models on the ID-Val. The loss on different token positions follows a dynamic hyperbolic-law.

hyperbolic-law. The conclusion still holds when evaluated on the OOD-Val. We leave those results in the Appendix.

**From the Dynamic Hyperbolic-law to the Overall Temporal Pattern.** In the dynamic hyperbolic-law,  $a_2$  is the converging factor denoting the converged value of loss on each token as context length increases.  $a_0$  denotes the loss gap between the first token and the last token, and  $a_1$  is the scaling factor along sequence length. To analyze the temporal pattern of the overall test loss, we collect the tuple  $(a_0, a_1, a_2)$  for all evaluated steps during pre-training phase:  $[(a_0^{N_1}, a_1^{N_1}, a_2^{N_1}), \dots, (a_0^{N_{tot}}, a_1^{N_{tot}}, a_2^{N_{tot}})]$ , where  $N_i$  is the number of trained tokens at step  $i$ , and  $N_{tot}$  is the total number of tokens used for pre-training. We plot the original  $(a_0, a_1, a_2)$  data on ID-Val w.r.t. the number of tokens trained (denoted as  $N$ ) for the 468M model in Fig. 2. We fit the temporal evolution of  $a_0$ ,  $a_1$ , and  $a_2$  factors to depict the overall temporal test loss pattern.

Empirically, we use the following functions to fit for  $a_0$  and  $a_1$ :

$$\begin{aligned} a_0^N &= \alpha_0 \log(\alpha_1 \log(N) + \alpha_2) + \alpha_3, \\ a_1^N &= \frac{\beta_0}{1 + \beta_1 N} + \beta_2, \end{aligned} \quad (6)$$

where the  $\{\alpha_i\}$  and  $\{\beta_i\}$  fitting parameters are solved by non-linear least squares. Observed from the original data in Fig. 2, we find that the value of  $a_0$  and  $a_1$  generally converges after a period of training, but suffer from fluctuations after converging due to the uncertainty of the first prediction position in a sequence. To mitigate the fluctuations,

we define a separation point  $N_{sep}$ :

$$N_{sep} := \min N, \text{ s.t. } \nabla a_0^N < \epsilon, \nabla a_1^N < \epsilon. \quad (7)$$

We manually stabilize the values of  $a_0$  and  $a_1$  after  $N_{sep}$ :

$$a_0^N = a_0^{N_{sep}}, a_1^N = a_1^{N_{sep}}, (N \geq N_{sep}). \quad (8)$$

We empirically set  $\epsilon = 10^{-4}/1\text{B}$  tokens.

For parameter  $a_2$ , we utilize the separation point  $N_{sep}$  to analyze its temporal pattern. We observe that  $N_{sep}$  is also a separation point for  $a_2$ , as it marks the shift of its decrease pattern. Before  $N_{sep}$ , we apply the same function form of the loss gap factor  $a_0$  as in Eq. (6). After  $N_{sep}$ , we find that its temporal pattern holds strong correlations with the cosine learning rate scheduler, and in turn apply a cosine relation. As a result, we find that  $a_2$  can be fit with a combination of the cosine and the logarithmic functions:

$$a_2^N = \begin{cases} \gamma_0 \log(\gamma_1 \log(N) + \gamma_2) + \gamma_3, & (N < N_{sep}) \\ \gamma_4 \cos(\gamma_5 N + \gamma_6) + \gamma_7, & (N \geq N_{sep}) \end{cases} \quad (9)$$

where  $\{\gamma_i\}$  are fitting parameters solved by non-linear least squares. From the fit for  $a_2$ , we find that  $\gamma_5 \approx \frac{\pi}{N_{tot}}$ , indicating that the training schedule resembles half of a cosine period, which is consistent to the setting of the cosine scheduler. It further validates our speculation that  $a_2$  has a strong correlation with the cosine learning rate decay.

We plot the fit of  $a_0$ ,  $a_1$ , and  $a_2$  in Fig. 2. We can observe that our fit captures the primary patterns of parameter evolution and ignores the insignificant fluctuations. We leave further results on the OOD-Val and the 1.2B model in the Appendix.

After acquiring  $a_0^N$ ,  $a_1^N$ , and  $a_2^N$ , we could in turn measure the pattern of the total test loss  $\mathcal{L}_N$  by averaging the loss on each token:

$$\mathcal{L}^N = \frac{1}{n} \sum_{i=1}^n \frac{a_0^N}{1 + a_1^N \cdot i} + a_2^N. \quad (10)$$

As listed in Tab. 1, the fit for all ground-truth test losses during the whole training process achieves  $R^2 > 0.99$  across different settings, demonstrating the validity of our temporal scaling law.

**Summary.** Overall, we summarize our temporal scaling law as follows:

- For LLM pre-training, in each training step, the loss for tokens in different positions follows a dynamic hyperbolic-law, in which parameters change as training steps increase.

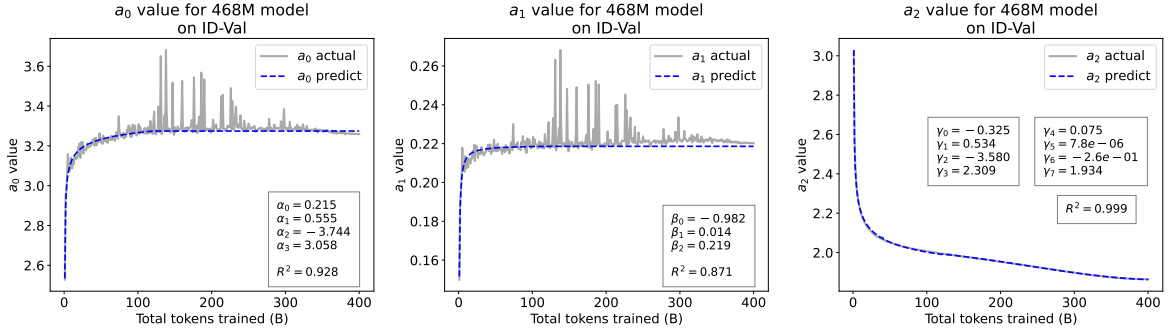


Figure 2: The fitting curve for  $a_0$ ,  $a_1$ , and  $a_2$  on ID-Val throughout the pre-training stage of the 468M model.

- The temporal patterns (i.e., values in different training steps) of dynamic hyperbolic-law parameters can be captured individually.
- The temporal pattern of the overall test loss is derived by averaging losses at all token positions acquired by the dynamic hyperbolic-law.

### 3.4 Test Loss Prediction

The primary value of scaling laws lies in their capability of predicting training outcomes (Kaplan et al., 2020). From the temporal perspective, accurate predictions towards the upcoming training periods can assist in a direct selection of hyperparameters based on the target LLM’s performance, early stopping, etc. In this section, we derive practical methods from our temporal scaling law to accurately predict the overall loss in the upcoming training periods using data from an early training period to derive parameters of the temporal scaling law, during which only  $N_{train}$  tokens are trained.

To predict the overall loss, we first predict the temporal trajectory of  $a_0^N$ ,  $a_1^N$ , and  $a_2^N$ . We could fit for  $a_0^N$  and  $a_1^N$  with the functions in Eq. (6)<sup>1</sup>:

$$\begin{aligned} \tilde{a}_0^N &= \tilde{\alpha}_0 \log(\tilde{\alpha}_1 \log(N) + \tilde{\alpha}_2) + \tilde{\alpha}_3, \\ \tilde{a}_1^N &= \frac{\tilde{\beta}_0}{1 + \tilde{\beta}_1 N} + \tilde{\beta}_2, \end{aligned} \quad (11)$$

where  $\{\tilde{\alpha}_i\}$  and  $\{\tilde{\beta}_i\}$  are fit using  $\{\mathcal{L}_i^N\}$  ( $N < N_{train}$ ) with non-linear least squares. Following Eq. (7), we could estimate the separation point as  $\tilde{N}_{sep}$ . Based on the relationship of  $N_{train}$  and  $\tilde{N}_{sep}$ , the test loss is predicted in different ways:

**Situation #1:**  $N_{train} \leq \tilde{N}_{sep}$ . For  $\tilde{a}_0^N$  and  $\tilde{a}_1^N$ , we apply the fit Eq. (11) for  $N \leq \tilde{N}_{sep}$ . For  $\tilde{a}_2^N$ , we first fit the first segment in Eq. (9):

$$\tilde{a}_2^N = \tilde{\gamma}_0 \log(\tilde{\gamma}_1 \log(N) + \tilde{\gamma}_2) + \tilde{\gamma}_3, \quad (12)$$

<sup>1</sup>To mitigate the effect of fluctuations, we filter outliers based on the first-fit residuals and re-fit for the final result.

where  $\{\gamma_i\}$  are fit using non-linear least squares. Due to the absence of test loss data for  $N_{train} > \tilde{N}_{sep}$ , we could not acquire the value for  $\tilde{a}_0^N$ ,  $\tilde{a}_1^N$ , and  $\tilde{a}_2^N$  at that period directly. To estimate the patterns after the separation point, we propose general boundary conditions for estimation:

$$\begin{aligned} \frac{d\tilde{a}_i^N}{dN} \Big|_{N \rightarrow \tilde{N}_{sep}^+} &= \frac{d\tilde{a}_i^N}{dN} \Big|_{N \rightarrow \tilde{N}_{sep}^-}, \\ \tilde{a}_i^{N \rightarrow \tilde{N}_{sep}^+} &= \tilde{a}_i^{N \rightarrow \tilde{N}_{sep}^-}. \end{aligned} \quad (13)$$

According to the definition in Eq. (7), we simply stabilize the values for  $\tilde{a}_0^N$  and  $\tilde{a}_1^N$  as  $\tilde{a}_0^{\tilde{N}_{sep}}$  and  $\tilde{a}_1^{\tilde{N}_{sep}}$  correspondingly for  $N > \tilde{N}_{sep}$ , fulfilling the derivative condition in Eq. (13) approximately. For  $\tilde{a}_2^N$  at  $N \geq \tilde{N}_{sep}$ , to eliminate the number of unknown variables, we directly adopt the discovery from fitting Eq. (9) that  $a_2$  is strongly correlated with the learning rate schedule, and directly set  $\tilde{\gamma}_5 = \frac{\pi}{N_{tot}}$  and  $\tilde{\gamma}_6 = -\frac{\pi}{N_{tot}}N_w$ , where  $N_w$  is the number of tokens used for warmup training. We in turn solve for the rest parameters  $\tilde{\gamma}_4$  and  $\tilde{\gamma}_7$  in the following function based on Eq. (13):

$$\tilde{a}_2^N = \tilde{\gamma}_4 \cos\left[\frac{\pi}{N_{tot}}(N - N_w)\right] + \tilde{\gamma}_7. \quad (14)$$

**Situation #2:**  $N_{train} > \tilde{N}_{sep}$ : For  $\tilde{a}_0^N$  and  $\tilde{a}_1^N$ , we simply stabilize their values as in Situation #1. For  $\tilde{a}_2^N$ , we first acquire the fitting results for Eq. (14) following Situation #1. We then calibrate  $\tilde{\gamma}_4$  and  $\tilde{\gamma}_7$  with the  $N_{train} > \tilde{N}_{sep}$  data by estimating  $\epsilon_4$  and  $\epsilon_7$  using non-linear least squares:

$$\tilde{a}_2^N = (\tilde{\gamma}_4 + \epsilon_4) \cos\left[\frac{\pi}{N_{tot}}(N - N_w)\right] + (\tilde{\gamma}_7 + \epsilon_7). \quad (15)$$

After acquiring the complete estimations of  $\tilde{a}_0^N$ ,  $\tilde{a}_1^N$ , and  $\tilde{a}_2^N$ , we could calculate the test loss prediction  $\tilde{\mathcal{L}}_N$  for each training step with Eq. (10).

**Experiments.** The prediction for test losses in upcoming training periods is a time series modeling

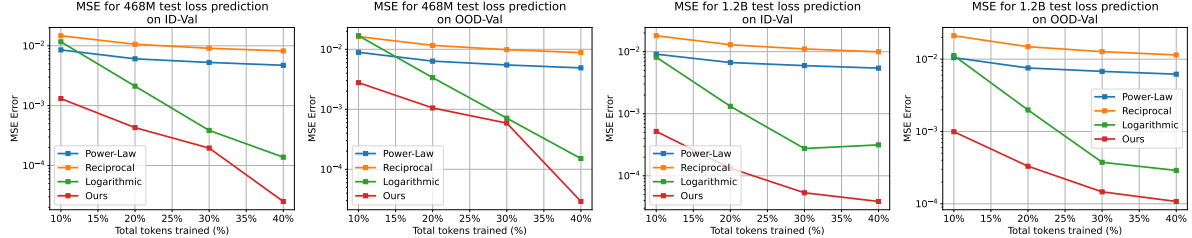


Figure 3: MSE results for predicting the subsequent test loss via the temporal scaling law after completing different proportions of the training process. Note that the y-axis representing the MSE error is in log scale.

problem where no ground-truth data is provided. Following the standard practice of time series modeling (Wu et al., 2021; Liu et al., 2022), we choose the MSE metric to evaluate the predictions:

$$\text{MSE} = \frac{1}{n} \sum_{i=1}^n (\mathcal{L}_i - \tilde{\mathcal{L}}_i)^2. \quad (16)$$

Apart from the power-law, we also choose the reciprocal ( $\mathcal{L} = \frac{a_0}{1+a_1N} + a_2$ ) and the logarithmic ( $\mathcal{L} = \log(a_1 + a_2N) + a_3$ ) relations as baselines that model the test loss as a whole. We predict the subsequent test loss after deriving parameters of the temporal scaling law from, respectively, 10%, 20%, 30%, and 40% of the training process. As shown in Fig. 3, on different model scales and data budgets, while the baselines hardly generate reliable results, our method yields accurate results with  $\text{MSE} < 10^{-3}$  in most cases. Our method yields far better  $R^2$  as well. For example, when using 10% data for 1.2B model on ID-Val, our method yields  $R^2 = 0.87$ , while the power-law, reciprocal, and logarithmic baselines yield  $R^2 = -1.26, -3.47, -1.02$ , correspondingly. The prediction results provide strong evidence for the reliability of our temporal scaling law.

#### 4 Use Case #1 of Temporal Scaling Law: Hyperparameter Selection

Our temporal scaling law can be applied to enable a direct hyperparameter selection for LLMs. For example, data mixture proportions greatly affect the performance of LLMs (Touvron et al., 2023a,b; Xie et al., 2023a). Due to the huge computation cost of training with multiple data proportions directly on target LLMs, prior art simply applies the proportion values tuned on a much smaller model (Xie et al., 2023a). Using the temporal scaling law, we could accurately predict the final performance (in terms of test losses) of different data proportions without completing the extensive pre-training.

		ID-Val	OOD-Val
468M	Small Model / 10B Test Loss	8.65	11.92
	Our pipeline	<b>8.58</b>	<b>11.77</b>
1.2B	Small Model / 10B Test Loss	7.55	10.29
	Our pipeline	<b>7.50</b>	<b>10.17</b>

Table 2: Pre-trained model perplexity on our validation datasets. “Small Model” denotes the Top-1 on the smaller model. “10B Test Loss” denotes the Top-1 selected by real test loss after training 10B tokens. **Bold** represents the best result.

Specifically, recognizing that smaller models can still identify some effective, though suboptimal, hyperparameters, we employ a two-stage retrieval-rerank pipeline to select the best data mixture proportion for training a 468M/1.2B model. In the retrieval stage, following the prior art (Xie et al., 2023a), we use a small-scale model to locate a group of fairly good data mixture proportions. In the rerank stage, we train all located data proportions on the target LLM for acceptable training tokens, and locate the best one by predicting their final losses with our temporal scaling law.

**Experiment Setup.** In the retrieval stage, we conduct grid search on a 58M model and locate the Top-5 candidates. In the rerank stage, we train each proportion for 10B tokens before making the test loss prediction. To compare different data mixture proportions on the 468M/1.2B models, we primarily use the perplexity metric on the ID-Val and the OOD-Val. We also follow (Touvron et al., 2023a; Rae et al., 2021; Su et al., 2023) and employ 7 popular common sense reasoning benchmarks, including BoolQ (Clark et al., 2019), HellaSwag (Zellers et al., 2019), OpenBookQA (Mihaylov et al., 2018), PIQA (Bisk et al., 2020), SIQA (Sap et al., 2019), StoryCloze (Mostafazadeh et al., 2016), and Winogrande (Sakaguchi et al., 2021) for evaluation. See Appendix for more implementation details.

**Experiment Result.** We compare the data mixture proportion selected by our retrieval-rerank

		BoolQ	HellaSwag	OpenBookQA	PIQA	SIQA	StoryCloze	Winogrande
468M	Small Model / 10B Test Loss	<b>58.70</b>	45.38	31.25	68.60	43.39	64.78	<b>54.93</b>
	Our pipeline	57.07	<b>45.98</b>	<b>33.68</b>	<b>69.36</b>	<b>44.01</b>	<b>64.88</b>	54.02
1.2B	Small Model / 10B Test Loss	56.25	54.13	34.25	72.20	42.11	69.05	59.83
	Our pipeline	<b>58.70</b>	<b>54.51</b>	<b>34.90</b>	<b>72.36</b>	<b>46.73</b>	<b>69.11</b>	<b>60.32</b>

Table 3: Average benchmark performance (0/1/5-shot) of models pre-trained on different data proportions. “Small Model” denotes the Top-1 on the smaller model. “10B Test Loss” denotes the Top-1 selected by real test loss after training 10B tokens. **Bold** represents the best result.

	Default	Practice	Head	Body	Tail
468M		<b>8.62</b>	<b>8.62</b>	8.66	8.63
1.2B		<b>7.52</b>	<b>7.52</b>	7.56	7.53

Table 4: ID-Val perplexity of models pre-trained on different weighting strategies. “Head” represents “Head suppression”, etc. **Bold** represents the best result.

pipeline with baselines (1) the Top-1 selected directly on the much smaller model and (2) the Top-1 selected by comparing the real test losses after training 10B tokens on 468M/1.2B model. We find that both (1) and (2) make the same choice from the Top-5 candidates, and our pipeline locates a different choice from them. As shown in Tab. 2, our choice achieves lower perplexity across all settings after completing pre-training (i.e., 400B tokens). Additionally, as shown in Tab. 3, our choice yields superior benchmark performance in 12 of 14 metrics. Consequently, while optimal hyperparameter selected on small models may not transfer to large models, our temporal scaling law allows for a more precise selection of training hyperparameters based on the candidates filtered out by small models.

## 5 Use Case #2 of Temporal Scaling Law: Revisit the Training Strategy

The temporal scaling law has afforded the possibility to study LLM pre-training in a finer granularity. As noted in Sec. 3.3, tokens on different positions possess a fundamental bias in learning difficulty. Specifically, head tokens are generally harder to predict than tail tokens. However, as suggested by Eqs. (6) and (8),  $a_0$  and  $a_1$  remains constant after the separation point. Therefore, for  $N > N_{sep}$ :

$$\frac{\partial \mathcal{L}_i^N}{\partial N} = \frac{\partial a_2}{\partial N}, \quad (17)$$

which is unrelated to token position  $i$ , suggesting that LLMs learn equally on different token positions. Considering the uniform learning dynamics across token positions, we hypothesize that the

default strategy for training generative language models, in which losses on tokens in all positions are simply averaged, is an effective solution.

To validate the hypothesis, we conduct LLM pre-training with three position-based weighting strategies: Head suppression, Body suppression, and Tail suppression. These strategies are attached only after the  $N_{sep}$  point. As shown in Tab. 4, despite being weighted on different token positions, all suppression strategies acquire comparable or slightly inferior results to the default practice, in which losses are simply averaged among positions. It indicates that weighting different tokens by position during LLM pre-training probably cannot yield better results than the default practice, further demonstrating that it is unnecessary to re-weight tokens by their positions during LLM pre-training, though different positions possess fundamental bias in learning difficulty. See Appendix for more implementation and analysis details.

## 6 Conclusion

Our research introduces the novel concept of Temporal Scaling Law for Large Language Models (LLMs), studying how the loss of an LLM evolve as the training steps scale up. We analyze the loss patterns on different token positions and discovered that these patterns conform to a dynamic hyperbolic-law. By studying the temporal evolution of the dynamic hyperbolic-law, we could properly fit and precisely predict the evolution of the LLM’s test loss, marking a significant improvement over baseline methods. Such capability is crucial for numerous possible applications. For hyperparameter selection, we provide a retrieval-rerank pipeline, in which our temporal scaling law can be paired with hyperparameter tuning methods for better hyperparameter selection based directly on the target LLM’s performance. For understanding LLM pre-training, we provide evidence supporting that LLMs uniformly optimize the losses across different token positions after an early training period.

## 7 Limitations.

Our work termed Temporal Scaling Law, pioneers the modeling of LLM pre-training from a temporal perspective. Although our temporal scaling law exhibits significant potential for both LLM research and application, limitations still exist. First, our temporal scaling law is derived from the mainstream structure of LLMs, the GPT-based decoder transformers. The applicability of our findings to other architectures, such as Mixture of Experts (MoE) models, remains to be explored. Furthermore, our research primarily focuses on the pre-training stage. The temporal patterns in other scenarios, such as transfer learning, are not covered. We leave further investigations of the above topics to our future research.

## References

Armen Aghajanyan, Lili Yu, Alexis Conneau, Wei-Ning Hsu, Karen Hambardzumyan, Susan Zhang, Stephen Roller, Naman Goyal, Omer Levy, and Luke Zettlemoyer. 2023. *Scaling laws for generative mixed-modal language models*. In *International Conference on Machine Learning, ICML 2023, 23-29 July 2023, Honolulu, Hawaii, USA*, volume 202 of *Proceedings of Machine Learning Research*, pages 265–279. PMLR.

Stella Biderman, Hailey Schoelkopf, Quentin Gregory Anthony, Herbie Bradley, Kyle O’Brien, Eric Hallahan, Mohammad Aflah Khan, Shivanshu Purohit, USVSN Sai Prashanth, Edward Raff, Aviya Skowron, Lintang Sutawika, and Oskar van der Wal. 2023. *Pythia: A suite for analyzing large language models across training and scaling*. In *International Conference on Machine Learning, ICML 2023, 23-29 July 2023, Honolulu, Hawaii, USA*, volume 202 of *Proceedings of Machine Learning Research*, pages 2397–2430. PMLR.

Yonatan Bisk, Rowan Zellers, Ronan Le Bras, Jianfeng Gao, and Yejin Choi. 2020. *PIQA: reasoning about physical commonsense in natural language*. In *The Thirty-Fourth AAAI Conference on Artificial Intelligence, AAAI 2020, The Thirty-Second Innovative Applications of Artificial Intelligence Conference, IAAI 2020, The Tenth AAAI Symposium on Educational Advances in Artificial Intelligence, EAAI 2020, New York, NY, USA, February 7-12, 2020*, pages 7432–7439. AAAI Press.

Tom B. Brown, Benjamin Mann, Nick Ryder, Melanie Subbiah, Jared Kaplan, Prafulla Dhariwal, Arvind Neelakantan, Pranav Shyam, Girish Sastry, Amanda Askell, Sandhini Agarwal, Ariel Herbert-Voss, Gretchen Krueger, Tom Henighan, Rewon Child, Aditya Ramesh, Daniel M. Ziegler, Jeffrey Wu, Clemens Winter, Christopher Hesse, Mark Chen, Eric Sigler, Mateusz Litwin, Scott Gray, Benjamin Chess, Jack Clark, Christopher Berner, Sam McCandlish, Alec Radford, Ilya Sutskever, and Dario Amodei. 2020. *Language models are few-shot learners*. In *Advances in Neural Information Processing Systems 33: Annual Conference on Neural Information Processing Systems 2020, NeurIPS 2020, December 6-12, 2020, virtual*.

C.-L. Cheng, Shalabh, and G. Garg. 2014. *Coefficient of determination for multiple measurement error models*. *Journal of Multivariate Analysis*, 126:137–152.

Mehdi Cherti, Romain Beaumont, Ross Wightman, Mitchell Wortsman, Gabriel Ilharco, Cade Gordon, Christoph Schuhmann, Ludwig Schmidt, and Jenia Jitsev. 2023. *Reproducible scaling laws for contrastive language-image learning*. In *IEEE/CVF Conference on Computer Vision and Pattern Recognition, CVPR 2023, Vancouver, BC, Canada, June 17-24, 2023*, pages 2818–2829. IEEE.

Aakanksha Chowdhery, Sharan Narang, Jacob Devlin, Maarten Bosma, Gaurav Mishra, Adam Roberts, Paul Barham, Hyung Won Chung, Charles Sutton, Sebastian Gehrmann, Parker Schuh, Kensen Shi, Sasha Tsvyashchenko, Joshua Maynez, Abhishek Rao, Parker Barnes, Yi Tay, Noam Shazeer, Vinodkumar Prabhakaran, Emily Reif, Nan Du, Ben Hutchinson, Reiner Pope, James Bradbury, Jacob Austin, Michael Isard, Guy Gur-Ari, Pengcheng Yin, Toju Duke, Anselm Levskaya, Sanjay Ghemawat, Sunipa Dev, Henryk Michalewski, Xavier Garcia, Vedant Misra, Kevin Robinson, Liam Fedus, Denny Zhou, Daphne Ippolito, David Luan, Hyeontaek Lim, Barret Zoph, Alexander Spiridonov, Ryan Sepassi, David Dohan, Shivani Agrawal, Mark Omernick, Andrew M. Dai, Thanumalayan Sankaranarayana Pillai, Marie Pellat, Aitor Lewkowycz, Erica Moreira, Rewon Child, Oleksandr Polozov, Katherine Lee, Zongwei Zhou, Xuezhi Wang, Brennan Saeta, Mark Diaz, Orhan Firat, Michele Catasta, Jason Wei, Kathy Meier-Hellstern, Douglas Eck, Jeff Dean, Slav Petrov, and Noah Fiedel. 2023. *Palm: Scaling language modeling with pathways*. *J. Mach. Learn. Res.*, 24:240:1–240:113.

Christopher Clark, Kenton Lee, Ming-Wei Chang, Tom Kwiatkowski, Michael Collins, and Kristina Toutanova. 2019. *Boolq: Exploring the surprising difficulty of natural yes/no questions*. In *Proceedings of the 2019 Conference of the North American Chapter of the Association for Computational Linguistics: Human Language Technologies, NAACL-HLT 2019, Minneapolis, MN, USA, June 2-7, 2019, Volume 1 (Long and Short Papers)*, pages 2924–2936. Association for Computational Linguistics.

Jacob Devlin, Ming-Wei Chang, Kenton Lee, and Kristina Toutanova. 2019. *BERT: pre-training of deep bidirectional transformers for language understanding*. In *Proceedings of the 2019 Conference of the North American Chapter of the Association for Computational Linguistics: Human Language Technologies, NAACL-HLT 2019, Minneapolis, MN, USA*,

June 2-7, 2019, Volume 1 (Long and Short Papers), pages 4171–4186. Association for Computational Linguistics.

William Fedus, Barret Zoph, and Noam Shazeer. 2022. **Switch transformers: Scaling to trillion parameter models with simple and efficient sparsity.** *J. Mach. Learn. Res.*, 23:120:1–120:39.

Leo Gao, Stella Biderman, Sid Black, Laurence Golding, Travis Hoppe, Charles Foster, Jason Phang, Horace He, Anish Thite, Noa Nabeshima, Shawn Presser, and Connor Leahy. 2021. **The pile: An 800gb dataset of diverse text for language modeling.** *CoRR*, abs/2101.00027.

Leo Gao, Jonathan Tow, Baber Abbasi, Stella Biderman, Sid Black, Anthony DiPofi, Charles Foster, Laurence Golding, Jeffrey Hsu, Alain Le Noac'h, Haonan Li, Kyle McDonell, Niklas Muennighoff, Chris Ociepa, Jason Phang, Laria Reynolds, Hailey Schoelkopf, Aviya Skowron, Lintang Sutawika, Eric Tang, Anish Thite, Ben Wang, Kevin Wang, and Andy Zou. 2023. **A framework for few-shot language model evaluation.**

Tom Henighan, Jared Kaplan, Mor Katz, Mark Chen, Christopher Hesse, Jacob Jackson, Heewoo Jun, Tom B. Brown, Prafulla Dhariwal, Scott Gray, Chris Hallacy, Benjamin Mann, Alec Radford, Aditya Ramesh, Nick Ryder, Daniel M. Ziegler, John Schulman, Dario Amodei, and Sam McCandlish. 2020. **Scaling laws for autoregressive generative modeling.** *CoRR*, abs/2010.14701.

Danny Hernandez, Jared Kaplan, Tom Henighan, and Sam McCandlish. 2021. **Scaling laws for transfer.** *CoRR*, abs/2102.01293.

Jared Kaplan, Sam McCandlish, Tom Henighan, Tom B. Brown, Benjamin Chess, Rewon Child, Scott Gray, Alec Radford, Jeffrey Wu, and Dario Amodei. 2020. **Scaling laws for neural language models.** *CoRR*, abs/2001.08361.

Yong Liu, Haixu Wu, Jianmin Wang, and Mingsheng Long. 2022. **Non-stationary transformers: Exploring the stationarity in time series forecasting.** In *Advances in Neural Information Processing Systems 35: Annual Conference on Neural Information Processing Systems 2022, NeurIPS 2022, New Orleans, LA, USA, November 28 - December 9, 2022*.

Ilya Loshchilov and Frank Hutter. 2017. **SGDR: stochastic gradient descent with warm restarts.** In *5th International Conference on Learning Representations, ICLR 2017, Toulon, France, April 24-26, 2017, Conference Track Proceedings*. OpenReview.net.

Ilya Loshchilov and Frank Hutter. 2019. **Decoupled weight decay regularization.** In *7th International Conference on Learning Representations, ICLR 2019, New Orleans, LA, USA, May 6-9, 2019*. OpenReview.net.

Todor Mihaylov, Peter Clark, Tushar Khot, and Ashish Sabharwal. 2018. **Can a suit of armor conduct electricity? A new dataset for open book question answering.** In *Proceedings of the 2018 Conference on Empirical Methods in Natural Language Processing, Brussels, Belgium, October 31 - November 4, 2018*, pages 2381–2391. Association for Computational Linguistics.

Nasrin Mostafazadeh, Nathanael Chambers, Xiaodong He, Devi Parikh, Dhruv Batra, Lucy Vanderwende, Pushmeet Kohli, and James F. Allen. 2016. **A corpus and evaluation framework for deeper understanding of commonsense stories.** *CoRR*, abs/1604.01696.

OpenAI. 2023. **GPT-4 technical report.** *CoRR*, abs/2303.08774.

Alec Radford, Karthik Narasimhan, Tim Salimans, Ilya Sutskever, et al. 2018. Improving language understanding by generative pre-training.

Alec Radford, Jeffrey Wu, Rewon Child, David Luan, Dario Amodei, Ilya Sutskever, et al. 2019. Language models are unsupervised multitask learners. *OpenAI blog*, 1(8):9.

Jack W. Rae, Sebastian Borgeaud, Trevor Cai, Katie Millican, Jordan Hoffmann, H. Francis Song, John Aslanides, Sarah Henderson, Roman Ring, Susanah Young, Eliza Rutherford, Tom Hennigan, Jacob Menick, Albin Cassirer, Richard Powell, George van den Driessche, Lisa Anne Hendricks, Maribeth Rauh, Po-Sen Huang, Amelia Glaese, Johannes Welbl, Sumanth Dathathri, Saffron Huang, Jonathan Uesato, John Mellor, Irina Higgins, Antonia Creswell, Nat McAleese, Amy Wu, Erich Elsen, Siddhant M. Jayakumar, Elena Buchatskaya, David Budden, Esme Sutherland, Karen Simonyan, Michela Paganini, Laurent Sifre, Lena Martens, Xiang Lorraine Li, Adhiguna Kuncoro, Aida Nematzadeh, Elena Gribovskaya, Domenic Donato, Angeliki Lazaridou, Arthur Mensch, Jean-Baptiste Lespiau, Maria Tsimpoukelli, Nikolai Grigorev, Doug Fritz, Thibault Sotiaux, Mantas Pajarskas, Toby Pohlen, Zhitao Gong, Daniel Toyama, Cyprien de Masson d'Autume, Yujia Li, Tayfun Terzi, Vladimir Mikulik, Igor Babuschkin, Aidan Clark, Diego de Las Casas, Aurelia Guy, Chris Jones, James Bradbury, Matthew J. Johnson, Blake A. Hechtman, Laura Weidinger, Iason Gabriel, William Isaac, Edward Lockhart, Simon Osindero, Laura Rimell, Chris Dyer, Oriol Vinyals, Kareem Ayoub, Jeff Stanway, Lorrayne Bennett, Demis Hassabis, Kory Kavukcuoglu, and Geoffrey Irving. 2021. **Scaling language models: Methods, analysis & insights from training gopher.** *CoRR*, abs/2112.11446.

Colin Raffel, Noam Shazeer, Adam Roberts, Katherine Lee, Sharan Narang, Michael Matena, Yanqi Zhou, Wei Li, and Peter J. Liu. 2020. **Exploring the limits of transfer learning with a unified text-to-text transformer.** *J. Mach. Learn. Res.*, 21:140:1–140:67.

Keisuke Sakaguchi, Ronan Le Bras, Chandra Bhagavatula, and Yejin Choi. 2021. **Winogrande: an adver-**

sarial winograd schema challenge at scale. *Commun. ACM*, 64(9):99–106.

Maarten Sap, Hannah Rashkin, Derek Chen, Ronan Le Bras, and Yejin Choi. 2019. **Socialqa: Commonsense reasoning about social interactions**. *CoRR*, abs/1904.09728.

Zhenpeng Su, Xing Wu, Xue Bai, Zijia Lin, Hui Chen, Guiguang Ding, Wei Zhou, and Songlin Hu. 2023. **Infoentropy loss to mitigate bias of learning difficulties for generative language models**. *CoRR*, abs/2310.19531.

Hugo Touvron, Thibaut Lavril, Gautier Izacard, Xavier Martinet, Marie-Anne Lachaux, Timothée Lacroix, Baptiste Rozière, Naman Goyal, Eric Hambro, Faisal Azhar, Aurélien Rodriguez, Armand Joulin, Edouard Grave, and Guillaume Lample. 2023a. **Llama: Open and efficient foundation language models**. *CoRR*, abs/2302.13971.

Hugo Touvron, Louis Martin, Kevin Stone, Peter Albert, Amjad Almahairi, Yasmine Babaee, Nikolay Bashlykov, Soumya Batra, Prajwal Bhargava, Shruti Bhosale, Dan Bikel, Lukas Blecher, Cristian Canton-Ferrer, Moya Chen, Guillem Cucurull, David Esiobu, Jude Fernandes, Jeremy Fu, Wenyin Fu, Brian Fuller, Cynthia Gao, Vedanuj Goswami, Naman Goyal, Anthony Hartshorn, Saghar Hosseini, Rui Hou, Hakan Inan, Marcin Kardas, Viktor Kerkez, Madian Khabsa, Isabel Kloumann, Artem Korenev, Punit Singh Koura, Marie-Anne Lachaux, Thibaut Lavril, Jenya Lee, Diana Liskovich, Yinghai Lu, Yuning Mao, Xavier Martinet, Todor Mihaylov, Pushkar Mishra, Igor Molybog, Yixin Nie, Andrew Poulton, Jeremy Reizenstein, Rashi Rungta, Kalyan Saladi, Alan Schelten, Ruan Silva, Eric Michael Smith, Ranjan Subramanian, Xiaoqing Ellen Tan, Binh Tang, Ross Taylor, Adina Williams, Jian Xiang Kuan, Puxin Xu, Zheng Yan, Iliyan Zarov, Yuchen Zhang, Angela Fan, Melanie Kambadur, Sharan Narang, Aurélien Rodriguez, Robert Stojnic, Sergey Edunov, and Thomas Scialom. 2023b. **Llama 2: Open foundation and fine-tuned chat models**. *CoRR*, abs/2307.09288.

Ashish Vaswani, Noam Shazeer, Niki Parmar, Jakob Uszkoreit, Llion Jones, Aidan N. Gomez, Łukasz Kaiser, and Illia Polosukhin. 2017. **Attention is all you need**. In *Advances in Neural Information Processing Systems 30: Annual Conference on Neural Information Processing Systems 2017, December 4-9, 2017, Long Beach, CA, USA*, pages 5998–6008.

Haixu Wu, Jiehui Xu, Jianmin Wang, and Mingsheng Long. 2021. **Autoformer: Decomposition transformers with auto-correlation for long-term series forecasting**. In *Advances in Neural Information Processing Systems 34: Annual Conference on Neural Information Processing Systems 2021, NeurIPS 2021, December 6-14, 2021, virtual*, pages 22419–22430.

Sang Michael Xie, Hieu Pham, Xuanyi Dong, Nan Du, Hanxiao Liu, Yifeng Lu, Percy Liang, Quoc V. Le, Tengyu Ma, and Adams Wei Yu. 2023a. **Doremi: Optimizing data mixtures speeds up language model pretraining**. *CoRR*, abs/2305.10429.

Sang Michael Xie, Hieu Pham, Xuanyi Dong, Nan Du, Hanxiao Liu, Yifeng Lu, Percy Liang, Quoc V. Le, Tengyu Ma, and Adams Wei Yu. 2023b. **Doremi: Optimizing data mixtures speeds up language model pretraining**. In *Advances in Neural Information Processing Systems 36: Annual Conference on Neural Information Processing Systems 2023, NeurIPS 2023, New Orleans, LA, USA, December 10 - 16, 2023*.

Greg Yang, Edward J. Hu, Igor Babuschkin, Szymon Sidor, Xiaodong Liu, David Farhi, Nick Ryder, Jakub Pachocki, Weizhu Chen, and Jianfeng Gao. 2022. **Tensor programs V: tuning large neural networks via zero-shot hyperparameter transfer**. *CoRR*, abs/2203.03466.

Rowan Zellers, Ari Holtzman, Yonatan Bisk, Ali Farhadi, and Yejin Choi. 2019. **Hellaswag: Can a machine really finish your sentence?** In *Proceedings of the 57th Conference of the Association for Computational Linguistics, ACL 2019, Florence, Italy, July 28- August 2, 2019, Volume 1: Long Papers*, pages 4791–4800. Association for Computational Linguistics.

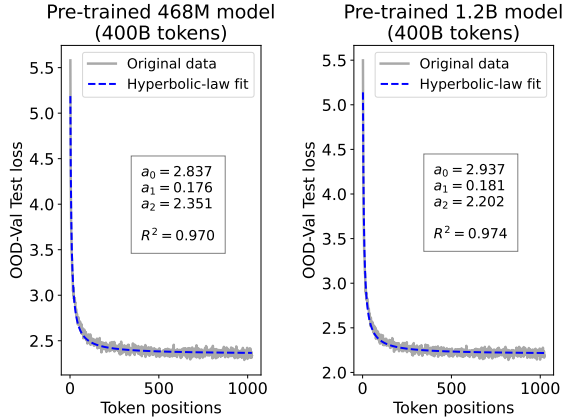


Figure 4: Graph of actual loss and fitting curve across different token positions for the 468M and 1.2B models on the OOD-Val.

## Appendix

### A Complete Fitting Results

As a supplement to Fig. 1, we provide fitting results of the dynamic hyperbolic-law on the OOD-Val for both the 468M and 1.2B models in Fig. 4. As a supplement to Fig. 2 in the article, we provide fitting results on both the ID-Val and the OOD-Val for both the 468M and 1.2B model scales in Fig. 5. Across different settings on model scales and validation set distributions, our temporal scaling law is able to depict the general trend of parameter evolution and reduce the influence of fluctuations as much as possible. By aggregating the temporal patterns on each token position through Eq. (10), our temporal scaling law is effective for modeling the overall training trajectory, reaching  $R^2 > 0.99$  for all settings, as shown in Tab. 1 in the article.

### B Further Experiment Details

In this section, we provide further experiment details towards the application cases in Sec. 4 and Sec. 5 in the article.

#### B.1 Additional General Information

Due to the page limit, we omitted some details for the general settings of our experiments. They are thoroughly described below for reproducibility.

**Evaluation Pipeline.** For all benchmark evaluations, we utilize the open-source LLM evaluation tool lm-evaluation-harness<sup>2</sup> (Gao et al., 2023), following (Su et al., 2023; Biderman et al., 2023).

<sup>2</sup><https://github.com/EleutherAI/lm-evaluation-harness>

For all numerical results, we report the average result tested on the last 5 checkpoints.

**License for Scientific Artifacts.** The Pile (Gao et al., 2021) is subject to the MIT license<sup>3</sup>. The C4 dataset (Raffel et al., 2020) is licensed under Open Data Commons License Attribution family<sup>4</sup>. The evaluation benchmarks (Gao et al., 2023) are subject to the MIT license. All usages of scientific artifacts in this paper obey the corresponding licenses.

**Hyperparameters of Models Used.** We report the details of model hyperparameters in Tab. 5.

**Parameters for Packages.** We report the version numbers of used packages in Tab. 6.

### B.2 More Experiment Setting Details for Hyperparameter Selection

Due to the page limit, we omitted some details for the experiment settings in Sec. 4. They are thoroughly described below for reproducibility.

**58M Model Construction.** The architecture of the 58M model is identical to the 70M parameter model outlined in (Biderman et al., 2023). The differences between model parameters can be ascribed to different vocabulary sizes and different activation functions (i.e., SwiGLU v.s. GeLU).

**Proportion Candidate Generation.** In the retrieval stage, we generate a group of proportion candidates by conducting grid search on domain weights in the Pile dataset (Gao et al., 2021). Specifically, we first calculate the original domain weight according to the original epoch settings noted by (Gao et al., 2021) on our applied 32k tokenizer. Note that *this is also the domain weight applied in Sec. 3.2*. For the grid search, we adopt a simple but popular pipeline by selecting a domain, modifying its domain weight by a random value  $s \in [-0.05, 0.05]$ , and normalizing the domain weight in other domains.

**Candidate Selection on the 58M Model.** In the retrieval stage, we choose the Top-5 data mixture proportions on the 58M model for the rerank stage and locate the Top-1 proportion on the 58M model for final comparisons. We choose the Top-5 and Top-1 proportions by calculating the average benchmark performance of the corresponding 58M model under 0-shot, 1-shot, and 5-shot settings.

<sup>3</sup><https://arxiv.org/pdf/2201.07311>

<sup>4</sup><https://huggingface.co/datasets/allenai/c4>

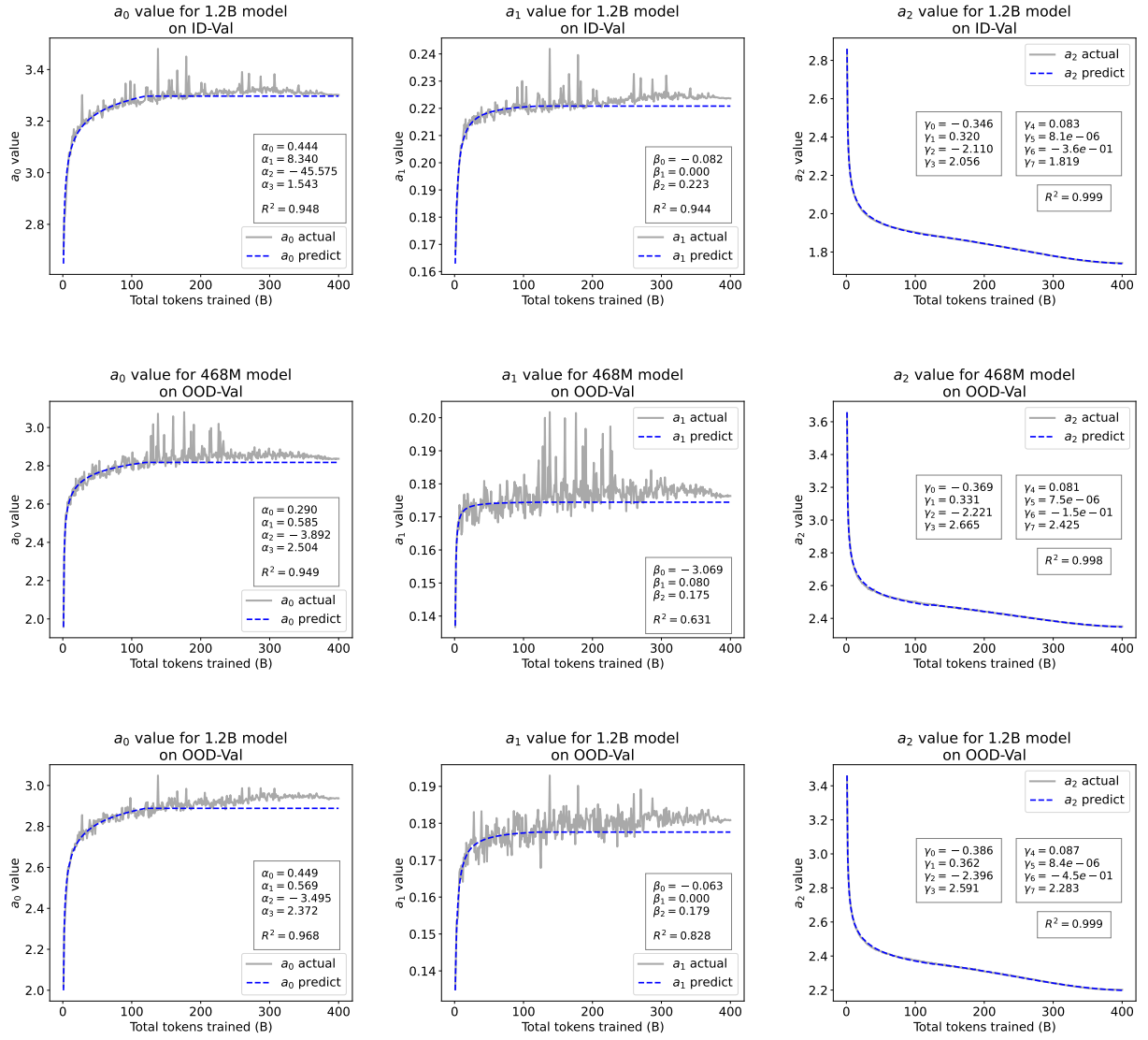


Figure 5: More fitting results for the 468M and the 1.2B models on both the ID-Val and OOD-Val.

model size	dimension	$n$ heads	$n$ layers	learning rate	scheduler	warmup	optimizer	batch size	seq length
58M	512	8	6	$3.0e^{-4}$	cosine	1k steps	AdamW	1024	1024
468M	1024	16	24	$3.0e^{-4}$	cosine	1k steps	AdamW	1024	1024
1.2B	2048	8	16	$3.0e^{-4}$	cosine	1k steps	AdamW	1024	1024

Table 5: Model sizes, architectures, and optimization hyperparameters.

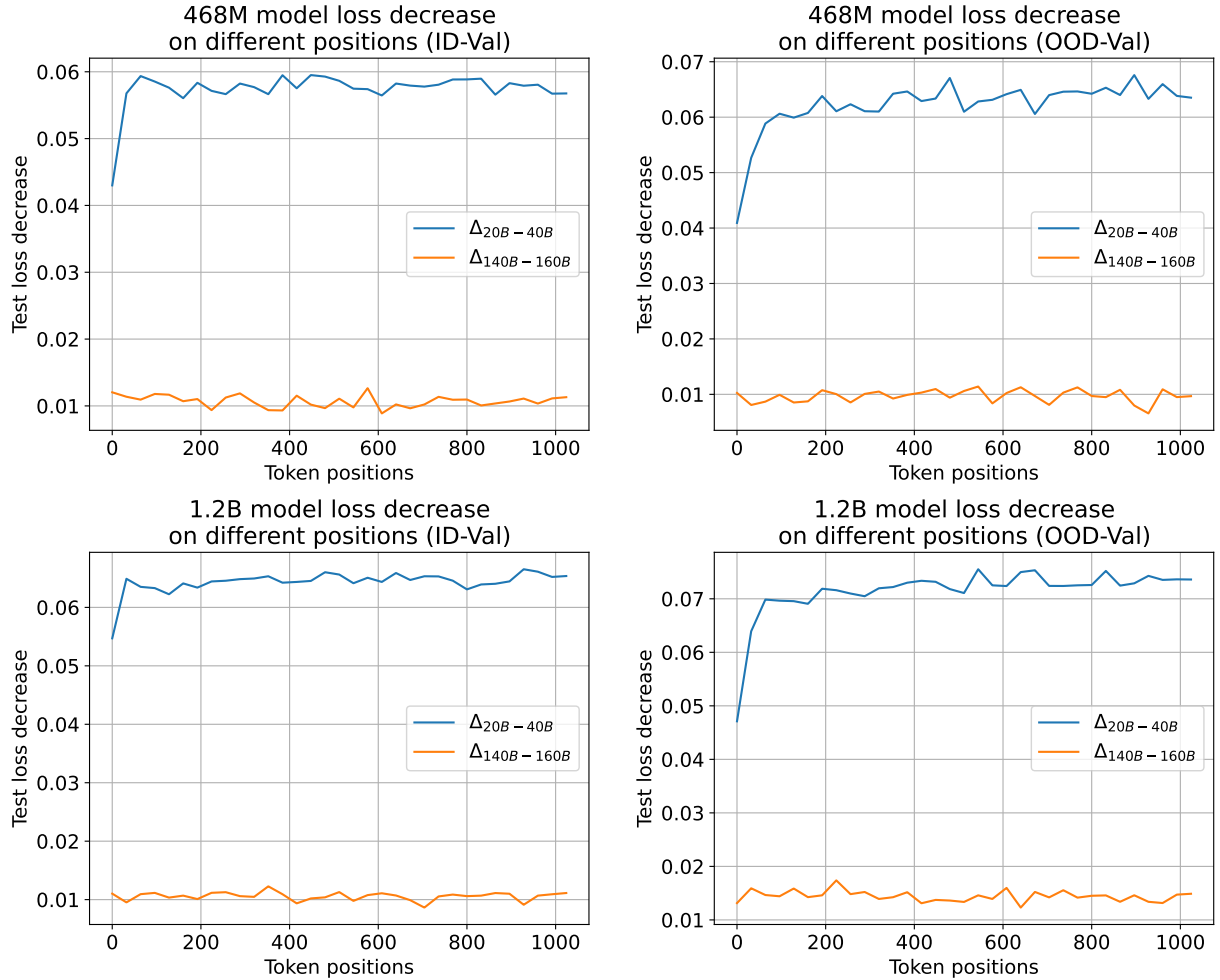


Figure 6: Test loss decrease on different token positions in the given training period for the 468M and the 1.2B models. “ $\Delta_{20B-40B}$ ” means the decrease of loss at each token position from “being trained with 20B tokens” to “being trained with 40B tokens” etc. After an early training period, the loss decrease tends to be uniform across all token positions (i.e.,  $\Delta_{140B-160B}$ ).

Package	Version	Package	Version
PyTorch	2.1.0	transformers	4.32.0
deepspeed	0.10.0	tokenizers	0.13.3
flash-attn	2.3.6	lm-evaluation-harness	0.3.0
datasets	2.14.3		

Table 6: Versions of used packages.

Strategy Name	Description
Default Practice	Average loss on all token positions.
Head Suppression	Weight loss on the foremost 10% tokens by 0.5x.
Body Suppression	Weight loss on the central 80% tokens by 0.5x.
Tail Suppression	Weight loss on the last 10% tokens by 0.5x.

Table 7: Details for different weighting strategies.

	BoolQ	HellaSwag	OpenBookQA	PIQA	SIQA	StoryCloze	Winogrande
468M	52.28	45.39	31.87	68.64	44.04	64.24	55.33
	52.05	<b>45.60</b>	31.80	68.50	<b>44.13</b>	<b>64.71</b>	55.38
	51.98	45.12	31.07	<b>68.66</b>	43.76	64.41	<b>55.64</b>
	<b>52.91</b>	45.28	31.67	68.05	44.03	<b>64.64</b>	55.62
1.2B	61.42	54.07	34.20	72.00	<b>45.87</b>	<b>68.63</b>	<b>58.64</b>
	59.96	<b>54.49</b>	34.33	71.75	45.36	68.39	<b>58.30</b>
	60.57	53.75	<b>34.80</b>	<b>72.05</b>	44.75	68.20	57.72
	<b>61.57</b>	54.02	<b>35.53</b>	71.49	<b>45.63</b>	<b>68.61</b>	58.27

Table 8: Average performance (0/1/5-shot) on common sense reasoning benchmarks of models pre-trained under different weighting strategies. **Bold** and underline represent the best and the second-best averaged results, correspondingly.

### B.3 More Observations for Token Position Loss

In Sec. 5, we have stressed that a fundamental bias in learning difficulty based on token position exists. Specifically, head tokens (with shorter context) are generally harder to predict than tail tokens (with longer context), due to the increased uncertainty caused by limited contextual information available for earlier tokens in a sequence. Surprisingly, our temporal scaling law suggests that LLMs learn equally on different token positions after an early training period (as shown by Eq. (17)), despite the learning difficulty bias.

**Observation for Actual Loss Decrease on Positions.** To validate this observation, we plot the actual loss decrease observed during training along different token positions in Fig. 6. As shown in Fig. 6, in the early training period of “from 20B to 40B tokens”, the head tokens suffer from less loss decrease due to a higher learning difficulty. However, after the early training period, in a later period of “from 140B to 160B tokens” that the separation point conditions in Eq. (7) are already fulfilled, test loss decrease among all token positions tends to be uniform across all settings. Therefore,

we can infer from this observation that the learning dynamics derived from our temporal scaling law are authentically presented in LLM pre-training.

**Details for Weighting Strategies.** In Sec. 5, we hypothesize that simply averaging the losses on all tokens is an effective solution for LLM pre-training. To validate the hypothesis, we have conducted LLM pre-training with three simple position-based weighting strategies. The implementation details of these strategies are described in Tab. 7. Note that for the Suppression strategies, we normalize the weighted losses to ensure the average weight for each token position is 1.0, and thus make the corresponding average loss comparable with the default practice. We apply the pre-training settings as in Sec. 3.2 for comparing different position-based weighting strategies.

**Benchmark Performance Observations.** In this paper, we have shown the effectiveness of the default practice from the perplexity perspective. To further validate that the default practice actually trains a competitive model compared to the weighting strategies, we test the model performance on the Common Sense Reasoning benchmark described in Sec. 4, and report average model performance

on 0-shot, 1-shot, and 5-shot settings. As shown in Tab. 8, all position-based weighting strategies acquire comparable or slightly inferior average results to the default practice, in which no weighting strategies are attached. On individual tasks, the default practice even achieves top-2 accuracies among 11 of 14 settings, surpassing all weighting variants. This indicates that weighting different tokens by position during LLM pre-training probably cannot yield better results than the default training strategy, further demonstrating that it is unnecessary to re-weight tokens by their positions during LLM pre-training.